CHAPTER IV

RESULTS AND DISCUSSION

4.1 Design-Expert Software

Design-Expert software was used to optimize the responses by providing the highly efficient design of experiments (DOE)

4.1.1 The 2-level Factorial Design

The most commonly used method in the experimental design involves the variation of one variable while keeping the other variables constant, until all variables have been studied. This methodology has two disadvantages; first, a large number of experiments are required, and second it is likely that the combined effect of two or more variables may not be identified (Deligiorgis et al., 2008). In this work, a statistical approach was chosen based on a factorial experimental design that would allow to inferring about the effect of the variables with a relatively small number of experiments. Fractional factorial can be used for screening many factors to find the significant ones where each factor is varied over 2 levels, high value and low value.

Electro-Fenton process was used as a main process to find the significant parameters or key parameters. The independent variables were pH, the amount of Fe^{2+} and H_2O_2 and current. The experimental design followed in this work was a full 2^4 experimental set, which required 16 experiments. The order of each experiment was selected and performed randomly. The values of the independent variables and the experiment data were shown in Table 4.1. The evaluation for correlation value of each factor was conducted and shown in Table 4.2. The correlation value was used to determine the key parameters that have possibility to affect on the responses which are OT and COD removal. From the correlation values, it indicates that pH, the amount of Fe^{2+} and H_2O_2 were the most important factors which can affect on OT and COD removal. As a result pH, Fe^{2+} and H_2O_2 were chosen as the key parameters. In addition, the meaning of minus sign for the correlation value of pH indicated that lower pH can give a positive effect on OT and COD removal. In contrast, the positive effect of $Fe^{2+}$and H_2O_2 concentration on OT and COD removal happened at higher value but OT removal efficiency did not significant change when applying the current from 1 to 4 A.

The experimental response (Y) associated to the three key parameters from 2k factorial design is represented by a linear polynomial model with interaction (Edelahi, 2004) as follows:

$$Y = b_0 + b_1X_1 + b_2X_2 + b_3X_3 + b_{12}X_1X_2 + b_{13}X_1X_3 + b_{23}X_2X_3 + b_{123}X_1X_2X_3 \quad (4.1)$$

These coefficients can be used to predict the influence of selected factor including pH (b_1), the amount of Fe^{2+} (b_2), H_2O_2 concentration (b_3), the interaction between pH and Fe^{2+} concentration (b_{12}), pH and H_2O_2 concentration (b_{13}), Fe^{2+} and H_2O_2 concentration (b_{23}) and the interaction between pH, Fe^{2+} and H_2O_2 concentration

Table 4.1: The result from 2-level factorial design

Run	Factor				Response	
	pH	Fe^{2+} (mM)	H_2O_2 (mM)	Current (A)	OT removal (%)	COD removal (%)
1	4.0	0.2	5.0	4.0	17	23
2	2.0	1.0	5.0	1.0	94.4	57
3	4.0	0.20	5.0	1.0	32	22
4	4.0	1.0	5.0	4.0	56	33
5	2.0	0.20	5.0	1.0	42	28
6	2.0	1.0	5.0	4.0	100	59.5
7	2.0	1.0	1.0	1.0	66.4	33
8	2.0	1.0	1.0	4.0	68.5	46
9	4.0	1.0	1.0	4.0	45	34
10	4.0	0.20	1.0	1.0	23	19
11	2.0	0.20	5.0	4.0	74	38.4
12	2.0	0.20	1.0	1.0	40	22.5
13	4.0	0.20	1.0	4.0	26.5	27
14	4.0	1.0	5.0	1.0	61.4	36
15	2.0	0.20	1.0	4.0	56.4	34.6
16	4.0	1.0	1.0	1.0	48	31

(b_{123}) on the OT or COD removal (Y). According to the results obtained, the final linear polynomial equations for the significant factors of OT and COD were formed by the software in term of actual factors as shown in equations (4.2) and (4.3), respectively.

Table 4.2: The correlation values of variable parameter

Factor	Correlation value	
	OT removal	COD removal
pH	-0.628	-0.517
Fe^{2+}	0.617	0.633
H_2O_2	0.278	0.274
Current	0.098	0.259

$$\text{OT removal} = 64.22 - 11.02\times pH + 12.36\times[Fe^{2+}] + 3.25\times[H_2O_2] + 2.73\times pH \times[Fe^{2+}] -1.02\times pH\times[H_2O_2] +8.58\times[Fe^{2+}]\times[H_2O_2] -1.17\times pH\times[Fe^{2+}]\times[H_2O_2] \quad (4.2)$$

$$\text{COD removal} = 30.16 - 2.31\times pH + 7.47\,[Fe^{2+}] + 0.84\times[H_2O_2] + 0.91\times pH \times [Fe^{2+}] - 2.81\times pH\times[H_2O_2] + 8.03\times[Fe^{2+}]\times[H_2O_2] - 1.81\times pH\times[Fe^{2+}]\times[H_2O_2] \quad (4.3)$$

The ANOVA analysis indicated that these three variables, pH, Fe^{2+} and H_2O_2 concentration, and their interactions were significant and played important roles in the OT oxidation and COD removal by electro-Fenton as summarized in Tables 4.3 and 4.4.

4.1.2 Box-Benhken Design

Box-Behnken Design provides a response surface formed from each numeric factor and can be varied over 3 levels. The data from previous, 2-level factorial design, including the center point of each factor were used to find the optimum condition and determine the coefficients for OT and COD removal. The independent variables and the experiment data were presented in Table 4.5. One ampere of current was applied in this scenario. The correlation values indicated that pH had the most pronounced effect on OT and COD removal. The amount of ferrous has comparable effect on these responses while H_2O_2 concentration has more effect on COD removal than mineralization of OT (Table 4.6). The final equation relationship between the responses function (OT and COD removal) and the key parameters can be determined by equations (4.4) and (4.5):

Table 4.3: ANOVA test for the response function Y_1 (OT removal)

Source	Sum of squares	df	Mean squares	F-value	p-value Prob > F
Model	7790.65	7	1112.95	11.10	0.0015
X_1 (pH)	3387.24	1	3387.24	33.78	0.0004
X_2 (Fe^{2+})	3271.84	1	3271.84	32.63	0.0004
X_3 (H_2O_2)	663.06	1	663.06	6.61	0.0330
$X_1 X_2$	1.56	1	1.56	0.016	0.9037
$X_1 X_2$	190.44	1	190.44	1.90	0.2055
$X_2 X_3$	262.44	1	262.44	2.62	0.1443
$X_1 X_2 X_3$	14.06	1	14.06	0.14	0.7178
Residual	802.07	8	100.26		
Cor Total	8592.72	15			

Table 4.4: ANOVA test for the response function Y_2 (COD removal)

Source	Sum of squares	df	Mean squares	F-value	p-value Prob > F
Model	1808.81	7	258.40	8.06	0.0043
X_1 (pH)	552.25	1	552.25	17.23	0.0032
X_2 (Fe^{2+})	826.56	1	816.56	25.79	0.0010
X_3 (H_2O_2)	155.00	1	155.00	4.84	0.0591
$X_1 X_2$	52.56	1	52.56	1.64	0.2362
$X_1 X_2$	119.90	1	119.90	3.74	0.0891
$X_2 X_3$	68.89	1	68.89	2.15	0.1808
$X_1 X_2 X_3$	33.64	1	33.64	1.05	0.3356
Residual	256.41	8	32.05		
Cor Total	2065.22	15			

Table 4.5: The results from Box-Benhken design

Run	Factor			Response	
	pH	Fe^{2+} (mM)	H_2O_2 (mM)	OT removal (%)	COD removal (%)
1	2.0	0.60	5.0	91.4	42
2	4.0	0.60	5.0	31.2	17.6
3	2.0	1.0	3.0	75	36
4	2.0	0.20	3.0	47.4	16.4
5	2.0	0.60	1.0	63.4	30
6	4.0	0.60	1.0	34	16
7	3.0	0.20	5.0	51	24
8	4.0	0.20	3.0	15	17
9	3.0	0.60	3.0	60	32
10	3.0	1.0	1.0	52	21
11	3.0	0.20	1.0	42.4	16.4
12	4.0	1.0	3.0	49.4	21.2
13	3.0	1.0	5.0	78	36

Table 4.6: The correlation value of significant factors

Factor	Correlation value	
	OT removal	COD removal
pH	-0.725	-0.593
Fe^{2+}	0.484	0.455
H_2O_2	0.294	0.408

$$OT\ removal = 78.74 - 18.45 \times pH + 30.81 \times Fe^{2+} + 3.74 \times H_2O_2\ ;(R^2 = 0.8462) \quad (4.4)$$

$$COD\ removal = 30.41 - 6.58 \times pH + 12.63 \times Fe^{2+} + 2.26 \times H_2O_2\ ;(R^2 = 0.7254) \quad (4.5)$$

From the solution obtained from the software as shown in Table 4.7, the condition number eight was selected as the optimum condition which is at pH 2 with the concentration of Fe^{2+} and H_2O_2 of 1 mM and 4.85 mM, respectively, and with the desirability 0.974.

Table 4.7: Solution predicts from the Design-Expert software

Number	pH	Fe^{2+} (mM)	H_2O_2 (mM)	OT removal (%)	COD removal (%)	Desirability
1	2.00	1.00	5.00	91.34	41.19	0.984
2	2.00	1.00	4.98	91.27	41.15	0.983
3	2.00	0.99	5.00	91.13	41.11	0.981
4	2.01	1.00	5.00	91.07	41.09	0.980
5	2.00	0.99	5.00	91.01	41.06	0.979
6	2.02	1.00	5.00	90.92	41.04	0.978
7	2.00	0.98	4.99	90.76	40.95	0.976
8	2.00	1.00	4.85	90.78	40.86	0.974
9	2.00	0.96	5.00	90.05	40.66	0.965
10	2.08	1.00	5.00	89.84	40.66	0.964
11	2.11	1.00	5.00	89.29	40.46	0.957
12	2.00	0.93	5.00	89.0	40.27	0.951
13	2.17	1.00	5.00	88.22	40.08	0.942
14	2.00	1.00	4.31	88.77	39.63	0.937
15	2.00	1.00	4.27	88.62	39.55	0.934
16	2.00	1.00	3.59	86.07	38.00	0.887
17	2.00	0.71	5.00	82.46	37.56	0.856
18	2.00	1.00	1.44	78.03	33.13	0.737

The obtained optimum pH is in good agreement with early reports (Ting et al., 2008; Lu et al., 2003; Chou et al., 1999; Sire´ s et al., 2007; Li et al., 2007; Qiang et al., 2003). The highest of the Fe^{2+} concentration was selected similar to several studies published that increased the amount of Fe^{2+} increasing the removal efficiency (Pignatello, 1992; Abdessalem et al., 2007; Sirés et al., 2007). The H_2O_2 concentration was selected at 4.85 mM. Ting et al. (2008) found that the increase in the removal efficiency was due to the increase in hydroxyl radical concentration as a result of the addition of H_2O_2. These results coincided with the results reported by Barbeni et al. (1987), Huang et al. (1993), Trapido et al. (1998), Benitez et al. (1999), Kwon et al. (1999), who observed positive effects of increasing of Fe^{2+} and H_2O_2 concentrations in the Fenton and photo-Fenton treatments of various chlorophenols and substituted phenols. However, for complete mineralization of organic compounds by Fenton's reagent, high doses of H_2O_2 and Fe^{2+} are generally needed because the regeneration of Fe^{2+} ion is relatively slow (Safarzadeh et al., 1996). One ampere of current was applied for electrolysis, photo-electrolysis, H_2O_2 with current and Fe^{2+} with current. The software predicted the removal efficiency for OT and COD removal of 91% and 41%, respectively, at the optimum condition.

4.2 Kinetic information

Table 4.8 presents an example for the comparison between two kinetic models which are first-order and second-order kinetics. Both kinetic models were used to fit the data in 2 ways, i.e., included (whole) or excluded (no initial) the initial step. Experimental data reveal that the degradation of OT occurred in two steps, i.e., the disappearance rate of OT was very rapid at the beginning but tailing off after the initial stage. The second rate law as shown in equation 4.6 can be simplified to explain these two reaction stages. At the initial step, OT and Fenton's reagent (directly related to •OH) were present at the high concentrations; hence, their changes in this initial stage could be assumed to be small compared to their initial concentrations. As a result, pseudo zero-order kinetics was obtained as shown in equation 4.7. On the other hand, only •OH concentration was steady in the second stage. This is because in the electro-Fenton process, the ·OH formation rate is controlled by the electrical current (controlled constantly at 1 A) developed during electrolysis (Guivarch et al., 2003); thus, Fe^{2+} was regenerated from Fe^{3+} at the constant rate and, as a consequence, the ·OH production rate was also constant in the second step. Under these conditions, the hydroxylation of OT became a pseudo first-order reaction (equation 4.8).

Table 4.8: The comparison of the kinetic rate constants for OT degradation

Reaction	First-order		Second-order	
	k (min^{-1})	R^2	k (L/mol min)	R^2
No initial	0.0094	0.9813	0.0217	0.9606
Whole	0.0098	0.9693	0.0219	0.9632

$$-\frac{d[OT]}{dt} = k[OT][\cdot OH] \quad (4.6)$$

$$-\frac{d[OT]}{dt} = k'_{obs} \quad (4.7)$$

$$-\frac{d[OT]}{dt} = k''_{obs}[OT] \quad (4.8)$$

Where "k", "k'_{obs}" and "k''_{obs}" are intrinsic (L mol^{-1} min^{-1}), observed pseudo-zero order (mM min^{-1}), and observed pseudo-first order rate constant (min^{-1}), respectively.

4.2.1 Effect of pH

The OT and COD removal increased as the initial pH of solution decreased from 4 to 2 (Figures 4.1 and 4.2) and the kinetic rate constants, k_{obs} (Table 4.9), also decreased when increasing pH. This result relates with the correlation value from the software which had a minus sign meaning that the efficiency increased as the pH decreased. Similar results was found by Sun et al. (2007) who investigated the effect of pH on the kinetic rate constants for *p*-nitroaniline (PNA) degradation in the range of 2.0-6.0 . The value of k_{ap} quickly increased when pH increases from 2.0 to 3.0. They also indicated that the PNA degradation fits with the pseudo first-order kinetic model. Ting et al. (2008) who found that the poor degradation of 2,6-DMA at a high pH range which at 2-4 was optimum. It was caused by the formation of ferric and ferric hydroxide complexes with much lower catalytic capability than Fe^{2+}.

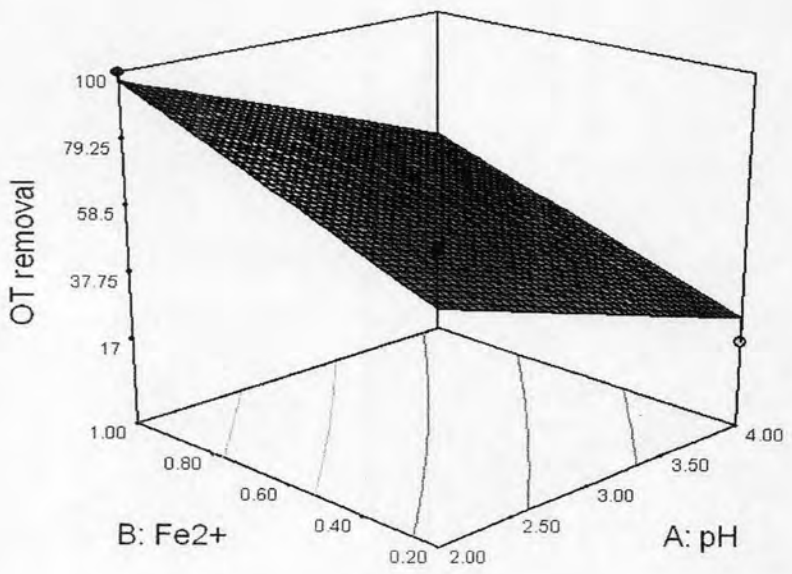

Figure 4.1: Variation of Fe^{2+} concentration and pH on OT removal

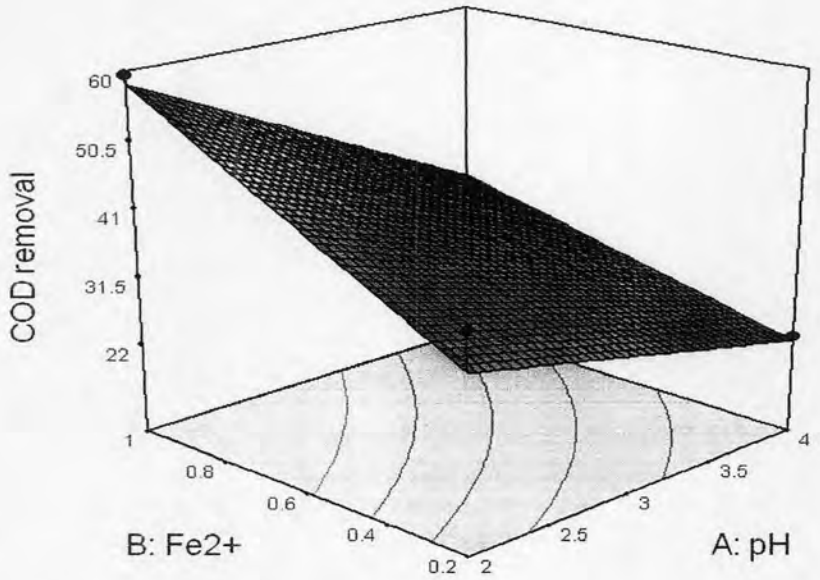

Figure 4.2: Variation of Fe^{2+} concentration and pH on COD removal of OT solution

4.2.2 Effect of Fe^{2+}

Ferrous concentration is another important factor that can enhance the removal efficiency when increased the concentration from 0.2 to 1 mM due to increasing in the reaction rate constant (Table 4.10). An increase in Fe^{2+} supplement was supposed to accelerate the ·OH generation rate and should consequently enhance the oxidation rate (Anotai et al., 2006). This result is supported by Katsumata et al. (2005) who found the degradation rate of linuron increased with increasing initial Fe^{2+} concentration and Sun et al. (2007) who found that the kinetic rate constant of PNA degradation was almost linearly increased with the increasing of Fe^{2+} concentration ($R > 0.98$). This is due to Fe^{2+} plays a very important role in initiating the decomposition of H_2O_2. Zuo and Hoigné (1992) found that at the first oxidation stages this catalyst caused an increase in degradation rate of contaminants, at times greater than 30 min the mineralization becomes very hard because of the formation of stable complexes of Fe^{3+} with oxalate and other short organic acids.

Table 4.9: Effect of pH on H_2O_2 efficiency and reaction rate (1.0 mM of [Fe^{2+}], 4.85 mM of [H_2O_2] and 1 A of current)

pH	k_{obs} (min^{-1})	H_2O_2 efficiency
2	0.0222	235.68
3	0.0057	147.26
4	0.0029	151.29

Table 4.10: Effect of Fe^{2+} on H_2O_2 efficiency and reaction rate (at pH 2, 4.85 mM of $[H_2O_2]$ and 1 A of current)

$[Fe^{2+}]$ (mM)	k_{obs} (min^{-1})	H_2O_2 efficiency
0.2	0.0036	110.95
0.6	0.0051	177.48
1.0	0.0222	235.68

The different result was found by Boye et al. (2003) and Brillas et al. (2007) who investigated the possible influence of Fe^{2+} concentration from 0.5 to 2.0 mM in the indirect electrooxidation methods. A gradual decay in TOC abatement, when Fe^{2+} concentration increased, led to a final mineralization of 86%, 80% and 70% for 0.5, 1.0 and 2.0 mM, respectively. This tendency can be accounted for by the slower degradation of pollutants due to the progressive waste of ·OH with increasing amount of Fe^{2+} by the non-oxidizing reaction (reaction 4.9) (Sun and Pignatello, 1993). A similar behavior was also found for the EF-Pt, EF-BDD and PEF-BDD treatments. Otherwise a large quantity of Fe^{3+} based sludge would be generated, which complicated the degradation due to the requirement of separation and disposal of the sludge (Sun et al., 2007).

$$Fe^{2+} + \cdot OH \rightarrow Fe^{3+} + OH^- \qquad (4.9)$$

4.2.3 Effect of H_2O_2

Several investigations have been reported an optimum peroxide concentration in the Fenton oxidation of dyes (Lin and Peng, 1995; Dutta et al., 2002) because unreacted H_2O_2 can act as a scavenger of ·OH and produces a less potent perhydroxyl radical, resulting in less efficiency of degradation. The degradation of OT and COD removals increased with increasing H_2O_2 concentration within the range of 1 to 5 mM. This can be explained by the effect of the additionally produced ·OH (Katsumata et al., 2005). Sun et al. (2007) also supported that the k_{ap} of PNA degradation increased with increase the initial H_2O_2 concentration in the range of 2.5-10 mM. However, with continuous increase of initial H_2O_2 concentration in the range of 10-40 mM, led to decline of k_{ap} especially when initial H_2O_2 concentration was higher 20 mM. This phenomenon could be explained from the perspective of so-called critical concentration of H_2O_2. Beyond the critical concentration, the degradation rate of organic compounds decreased with increasing of initial H_2O_2 concentration due to scavenging of ·OH by H_2O_2 and incremental generation of ·OOH which also consumed ·OH (Kang et al., 2002; Feng et al., 2003). Figure 4.3 shows that the efficiency of H_2O_2 decreased when increased H_2O_2 concentration. The similar result had been reported by Zhang et al. (2006) who found that efficiency of H_2O_2 decreased with the increase of Fenton's reagent dosage, indicating less H_2O_2 was used to degrade 4-nitrophenol. The efficiency of H_2O_2 could also exceed 100%. This is accounted for the fact that in electro-Fenton process, COD was removed by both oxidation and coagulation. The latter was due to the formation of ferric hydroxide

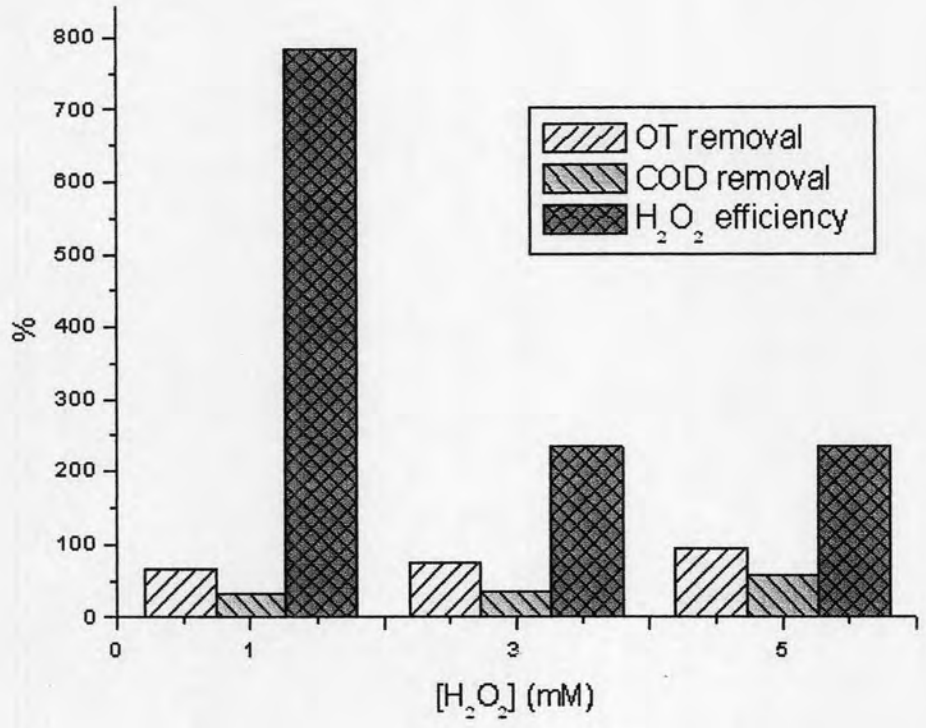

Figure 4.3: Effect of H_2O_2 on OT and COD removals and H_2O_2 efficiency (at pH 2, 1 mM of $[Fe^{2+}]$ and 1 A of current)

during neutralization step of electro-Fenton process. From the measure of COD during the reaction, the utilization efficiency of H_2O_2, E_H, can be calculated using equation (4.10) (Huang et al., 2001):

$$E_H\,(\%) = \frac{\text{actual COD removal}}{\text{theoretically removable COD by inlet } H_2O_2} \times 100\%$$

$$= \frac{COD_i - COD}{H_2O_2 \times 0.47} \times 100\% \qquad (4.10)$$

Where COD_i and COD denote the initial COD and the COD at time "t", respectively. H_2O_2 represents the dosage concentration of H_2O_2 at time "t". Tables 4.9 and 4.10 show the effect of pH and Fe^{2+} concentration on the H_2O_2 efficiency at constant reaction rate. Figures 4.4 and 4.5 also showed the OT and COD removal efficiencies. H_2O_2 efficiency and rate of reaction increased with decreasing of pH and increasing of Fe^{2+} concentration.

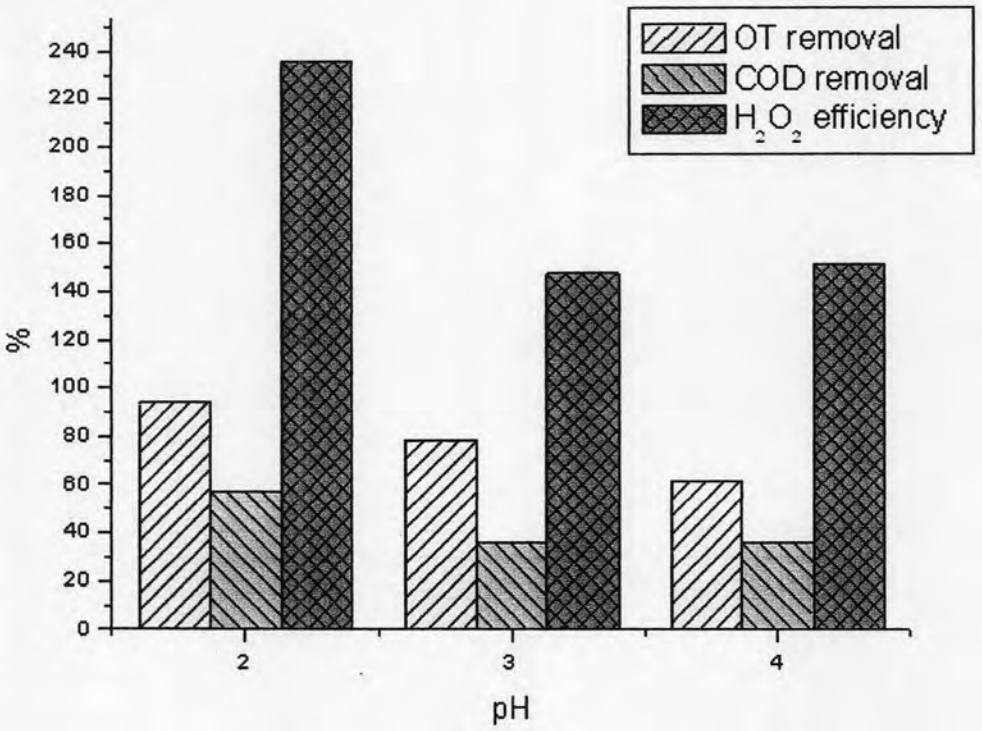

Figure 4.4: Effect of pH on OT and COD removals and H_2O_2 efficiency (1.0 mM of $[Fe^{2+}]$, 4.85 mM of $[H_2O_2]$ and 1 A of current)

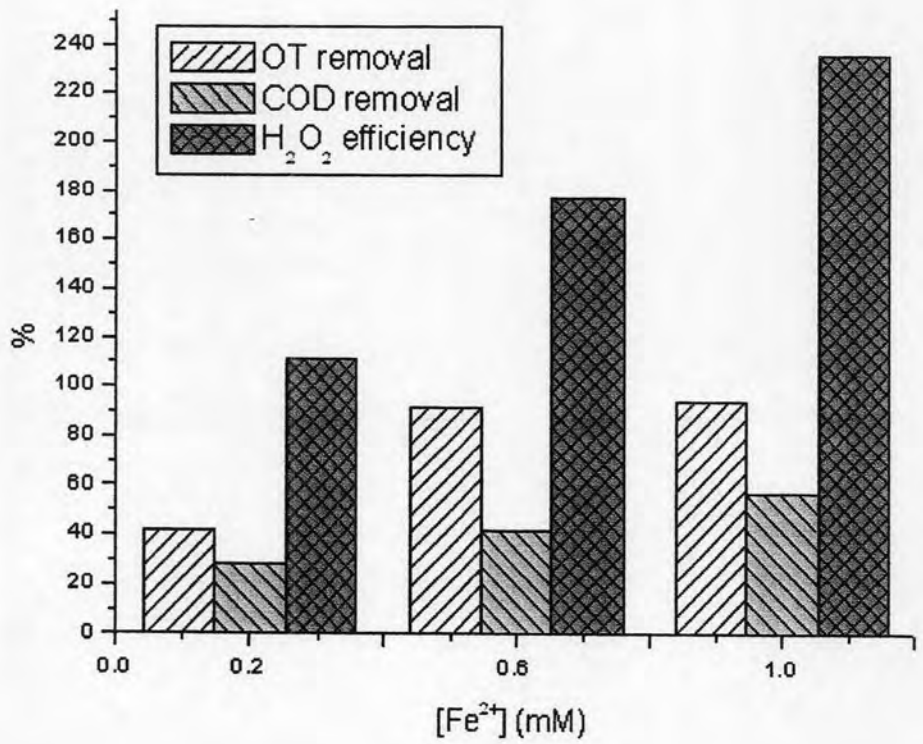

Figure 4.5: Effect of Fe^{2+} concentration on OT and COD removals and H_2O_2 efficiency (at pH 2, 4.85 mM of $[H_2O_2]$ and 1 A of current)

4.3 Control Experiments

All of parameters studied for the effect of each parameter including the synergistic possible effect between parameters in order to confirm the oxidation reaction, was from Fenton reaction. The results showed that all parameter and synergistic effect are not significant for the degradation of OT and COD abatement (Figures 4.6 and 4.7). Therefore, the optimum condition used for further study in the next scenarios. According to the study of Pignatello (1992) who found that no reaction occurred in control with H_2O_2 alone or Fe^{2+} alone and Goi and Trapido (2002) supported that the stirring of seven nitrophenols (NPs) with H_2O_2 without UV-radiation did not lead to the degradation of NPs. Direct UV-photolysis resulted in quite slow degradation of NPs with a pseudo-first order reaction rate constant about 10^{-5} s^{-1} that is not acceptable for practical application. The comparison of the data was complicated by different experimental condition in their studies (initial concentrations of NPs, H_2O_2 concentrations, temperature, pH, and especially, UV-radiation intensity and the type of UV-radiation source), which can differences in the degradation rate. Kajitvichyanukul et al. (2006) who also found that the degradation percentage of formaldehyde and methanol using UV alone were only 1.5 and 2%, respectively.

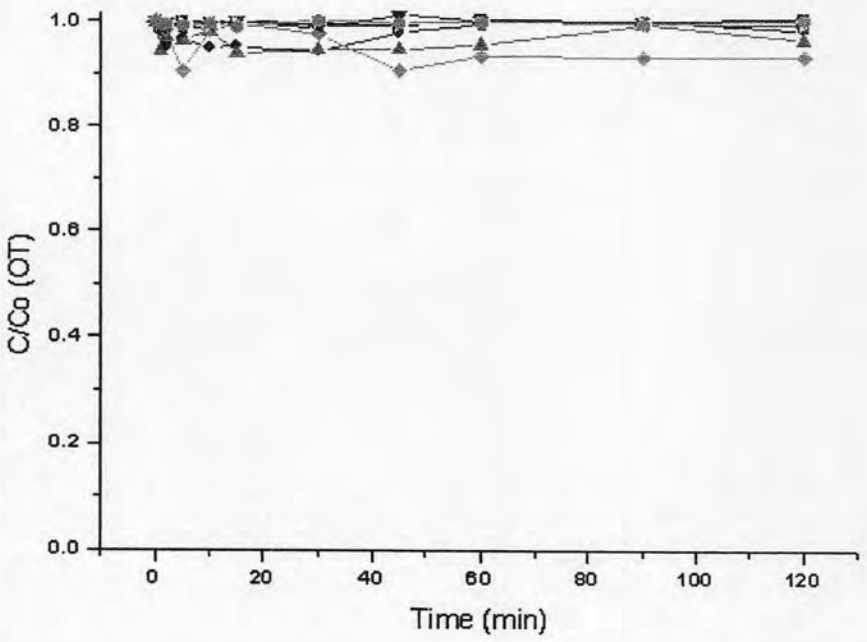

Figure 4.6: Effect of involving processes on OT abatement at pH 2; electrolysis (■); photolysis (✹); photo-electrolysis (▲); H_2O_2 (▼); H_2O_2 + UV (♦); H_2O_2 + current (◄); Fe^{2+} + current (►); Fe^{2+} + UV (●)

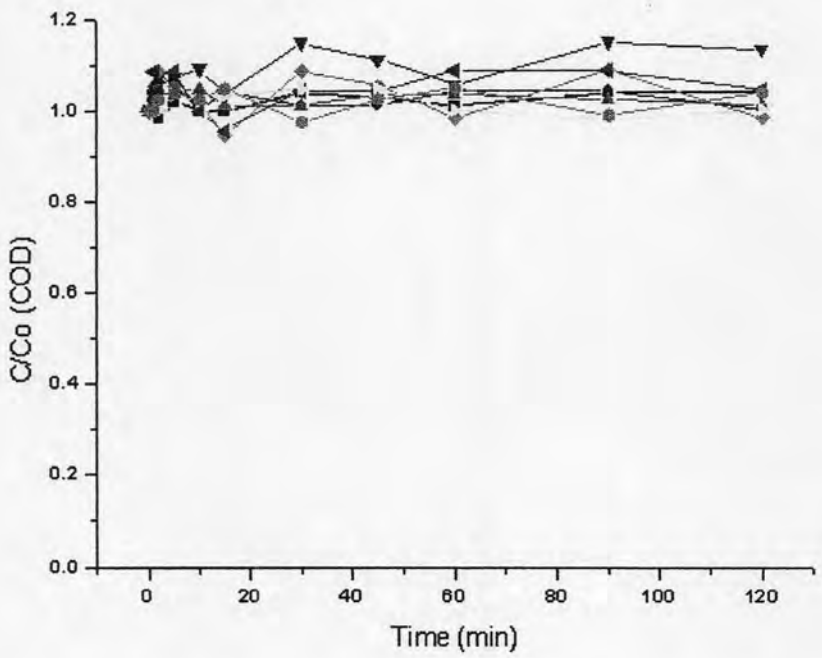

Figure 4.7: Effect of involving processes on COD reduction at pH 2; electrolysis (■); photolysis (✹); photo-electrolysis (▲); H_2O_2 (▼); H_2O_2 + UV (♦); H_2O_2 + current (◄); Fe^{2+} + current (►); Fe^{2+} + UV (●)

4.4 OT oxidation by several Fenton processes

·OH reacts with OT leading to its degradation. At the selected condition, 90% of OT was removed by Fenton process at treatment time of 2 hours. In Fenton oxidation processes, the rapid depletion of Fe^{2+} usually terminates the production of hydroxyl radicals (Lou and Lee, 1995; Saxe, et al., 2000; Qiang et al., 2000). For electro-Fenton, the OT was completely removed at 90 minutes which was higher than the removal efficiency that predicted by the software. Photoelectro-Fenton could degrade OT faster than that of electro-Fenton process with the same removal efficiency (100% at 60 minutes) because the irradiation of the hydroxylated Fe^{3+} or photoreduction of Fe^{3+} to Fe^{2+} (Balzani and Carassiti, 1970; Langford and Carey, 1975; Faust and Hoigné, 1990) could accelerate the production rate of hydroxyl radicals (Oturan and Brillas, 2007) which promoted the oxidation efficiency (Lu et al., 1999). The COD reduction by photoelectro-Fenton was greater than electro-Fenton, and Fenton i.e. 52, 50 and 36%, respectively. The COD abatement from the experiment was also higher than that of the software prediction. Based on the collected data, a mathematic model can be developed to estimate the required performances based on the selected reaction conditions, so that better cost-effectiveness can be achieved.

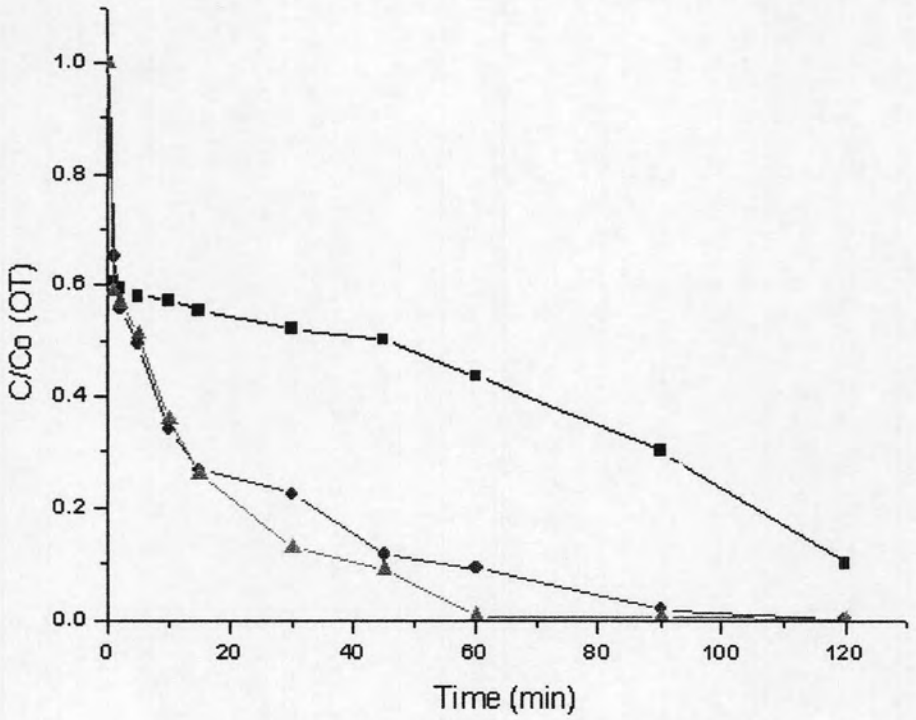

Figure 4.8: Degradation of OT at the optimum condition (at pH 2, $[Fe^{2+}]$ = 1 mM, $[H_2O_2]$ = 4.85 mM); Fenton (■); electro-Fenton (●); photoelectro-Fenton (▲)

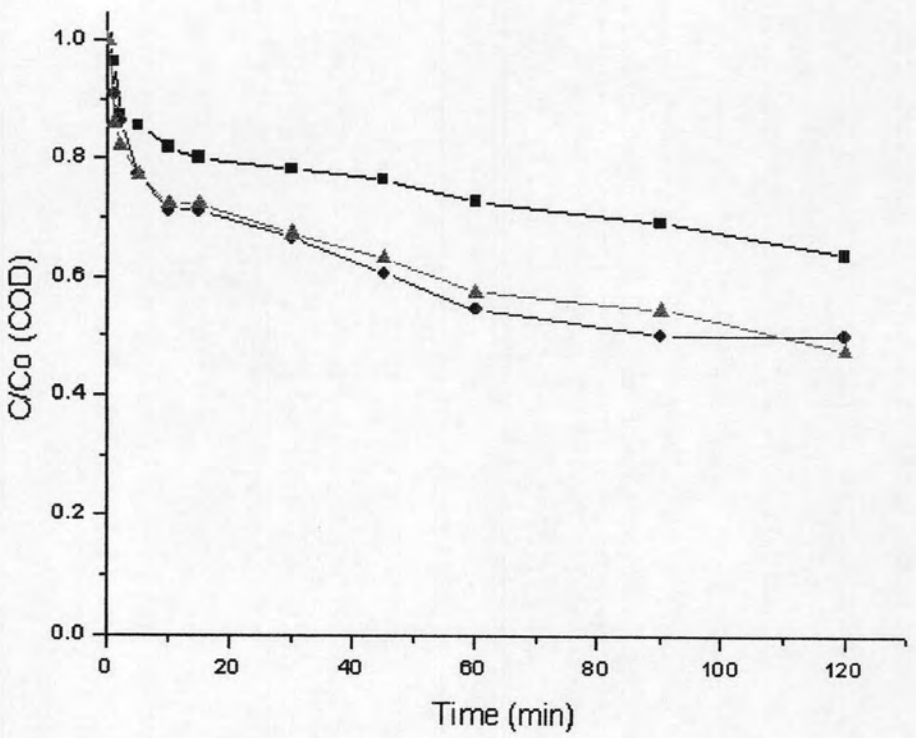

Figure 4.9: COD reduction at the optimum condition (at pH 2, $[Fe^{2+}]$ = 1 mM, $[H_2O_2]$ = 4.85 mM); Fenton (■); electro-Fenton (●); photoelectro-Fenton (▲)

4.5 Two stages reaction of OT decomposition

The degradation of OT could be divided into two-stage reaction. OT was swiftly degraded under the influence of Fe^{2+}/H_2O_2 reaction series. In the second stage, OT degraded slowly involving the Fe^{3+}/H_2O_2 reaction. This is similar to the previous work of Lu et al. (1999) who also found the two-stage reaction, i.e. the decomposition rate of dichlorvos before 30 seconds was far more rapid than that after 30 seconds. Malik and Saha (2003) also investigated the oxidation of direct dyes via the Fenton reaction and found that the entire degradation reaction could be divided into a two-stage reaction. In the first stage, referred to Fe^{2+}/H_2O_2 stage in which the dyes decomposed quickly; the second stage of reaction was referred to as the Fe^{3+}/H_2O_2 stage in which the decomposition rate became retarded.

In this study, the first stage reaction was explained by the initial rate, and the second stage was explained by the first order kinetic reaction. The reaction rate constants are listed in Table 4.11. As can seen that the initial rate between electro-Fenton and photoelectro-Fenton were comparable, these results may suggest that applying UV light at the early stage might not be necessary for a fast oxidation reaction of the electro-Fenton process. The similar result was found by Kajitvichyanukul et al. (2006) who investigated with Fenton and photo-Fenton processes.

4.6 Biodegradability of OT

The BOD_5/COD ratio constitutes an appropriate measure of the biodegradability of a wastewater. Accordingly, effluents with BOD_5/COD ratios exceeding 0.4 may be considered as readily biodegradable (Chamarro et al., 2001; Sarria et al., 2003). The effluent BOD_5/COD ratio increased from 0.125 by conventional Fenton process to 0.289 when apply with electric current or electro-Fenton process and to a greater extent of 0.357 when treated with photoelectro-Fenton process (Figure 4.10). This result indicated that electrical current and irradiation of UV light have an effect on the detoxicfication due to higher degradability and easilier biodegradable. Arslan and Gurses (2004) found that the BOD_5/COD ratio increased from 0.10 to 0.45 after the application of photo-Fenton-like process, but only to 0.24 after dark Fenton-like oxidation indicating that photo-Fenton- like pre-treatment of procaine penicillin G (PPG) formulation effluent is by far more effective in biodegradability improvement than the Fenton-like reaction and also inferred that photocatalytic reaction products seemed to be more biodegradable than those of the

Table 4.11: Reaction rate constant of OT oxidation by several Fenton processes

Process	1st stage reaction	2nd stage reaction
	Initial rate ($mM\ min^{-1}$)	k_{obs} (min^{-1})
Fenton	0.369	0.0124
Electro-Fenton	0.384	0.0356
Photoelectro-Fenton	0.389	0.0572

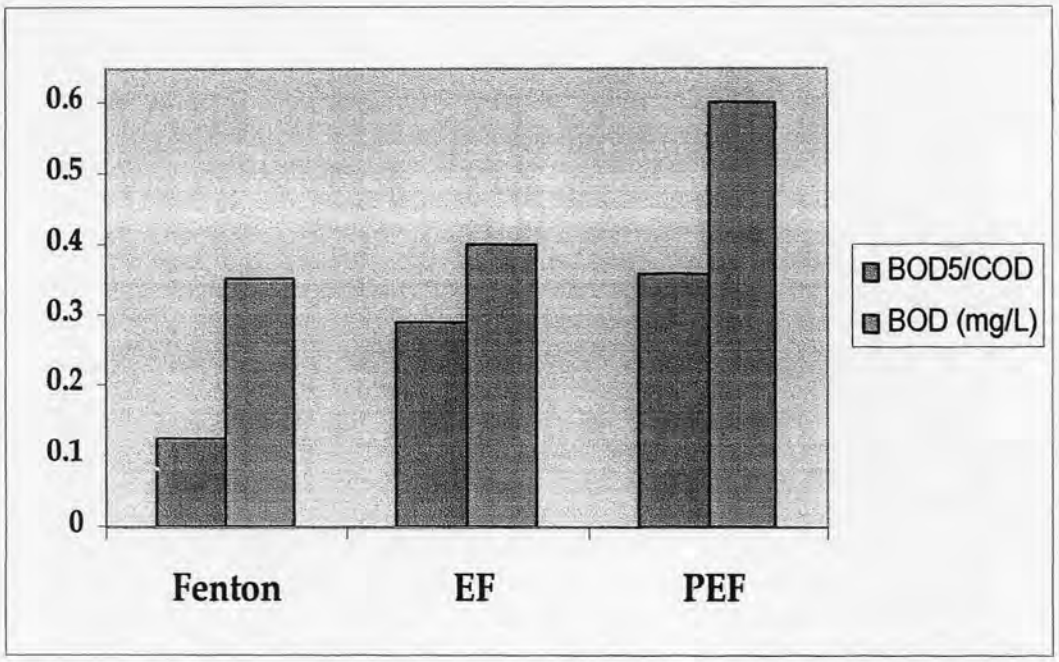

Figure 4.10: Toxicity reduction by various Fenton processes

dark Fenton-like process. In a related study, Sarria et al. (2003) investigated the oxidation of 5-amino-6-methyl-2-benzimidazolone (AMBI), an important precursor in the industrial production of dyes, by photo-assisted Fenton's reaction. It could be established that pre-treatment of AMBI produces completely mineralized by a succeeding biotreatment step.

4.7 Intermediate oxidation

Figures 4.11 and 4.12 showed that maleic and oxalic acids were identified as the intermediates from the oxidation of OT. These acids still increased until the end of the reaction period of ordinary Fenton experiment. In contrast, these products were much more quickly formed and destroyed under the electro-Fenton and photoelectro-Fenton degradations due to the greater generation of ·OH. In order word, it can be indicated that electro-Fenton and photoelectro-Fenton have higher efficiency to degrade organic acids than ordinary Fenton process. The accumulation of intermediates in photoelectro-Fenton process was lower than that of electro-Fenton process. Oxalic acid was slowly transformed to CO_2 by the two anodic oxidation, whereas in the indirect electro-oxidation treatments with iron ions, it mainly formed Fe^{3+}-oxalate complexes. These species are very stable in the electro-Fenton process (Boye et al., 2003). The fast destruction of these acids can be accounted by the efficient photodecomposition of its Fe^{3+} complexes under the action of UV light (Balzani and Carassiti, 1970; Zou and Hoigné, 1992). In addition, complexes of Fe^{3+} with carboxylic acids generated from the initial pollutants, such as oxalic acid, can be quickly photodecomposed into CO_2 with loss of Fe^{2+} as proposed by Zou and Hoigné (1992). The comparison of the TOC abatement between electro-Fenton and photoelectro-Fenton processes (Figure 4.13) found that 31% and 12% removal were obtained by photoelectro-Fenton and electro-Fenton, respectively.

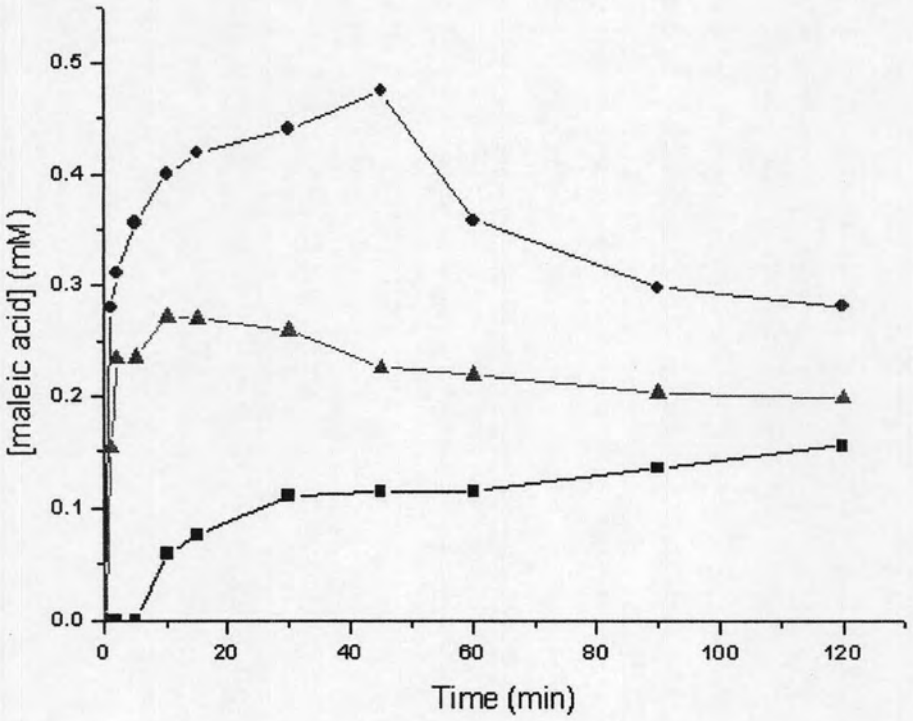

Figure 4.11: The oxidation of maleic acid by Fenton (■); electro-Fenton (●); photoelectro-Fenton (▲)

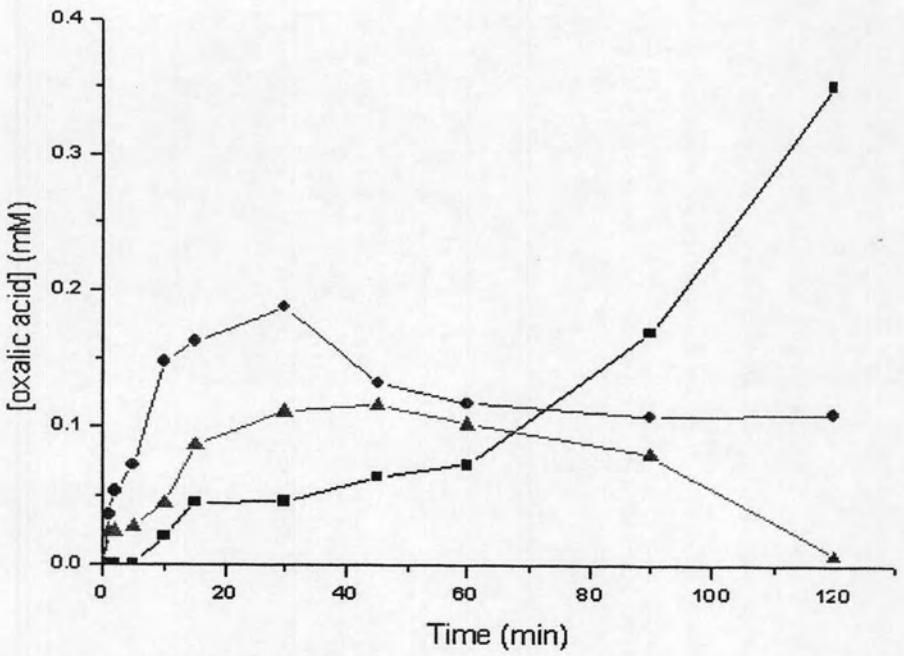

Figure 4.12: The oxidation of oxalic acid by Fenton (■); electro-Fenton (●); photoelectro-Fenton (▲)

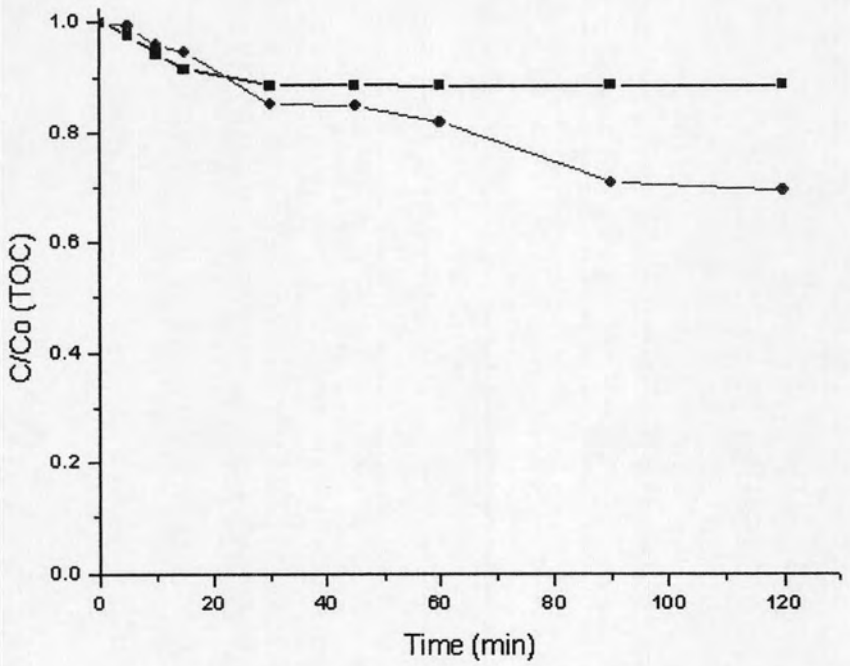

Figure 4.13: TOC abatement by electro-Fenton (■); photoelectro-Fenton (●)

Nevertheless, the complete mineralization of organic matters in term of COD and TOC did not occurred in all processes. The reduction of TOC and COD still proceeded after the disappearance of OT which implied that certain reactions still occurred in the solution as stated by Anotai et al. (2006). In addition, mass balance of carbon revealed that 50% of the carbon from OT was still in the solution in the organic forms representing by the COD value. Intermediates identified from OT oxidation by hydroxyl radicals were maleic and oxalic acids.